

Sustainable development of novel zinc oxide nano flowers mediated red yeast rice for control of hepatocellular carcinoma

Received: 17 July 2025

Accepted: 22 December 2025

Published online: 24 February 2026

Cite this article as: Jasim A.J., Yusop M.R., Taha B.A. *et al.* Sustainable development of novel zinc oxide nano flowers mediated red yeast rice for control of hepatocellular carcinoma. *Sci Rep* (2025). <https://doi.org/10.1038/s41598-025-33746-5>

Ahmed Jamal Jasim, Muhammad Rahimi Yusop, Bakr Ahmed Taha, Ahmed A. AL-Amiery, Noor Malik Saadoon, Muhammad Faheem Akhtar, Majid S. Jabir, Alaa Bassuny Ismael & Ayman A. Swelum

We are providing an unedited version of this manuscript to give early access to its findings. Before final publication, the manuscript will undergo further editing. Please note there may be errors present which affect the content, and all legal disclaimers apply.

If this paper is publishing under a Transparent Peer Review model then Peer Review reports will publish with the final article.

Sustainable Development of Novel Zinc Oxide Nano Flowers Mediated Red Yeast Rice for Control of Hepatocellular Carcinoma

Ahmed Jamal Jasim^{1,2}, Muhammad Rahimi^{2*}, Bakr Ahmed Taha³, Ahmed A. AL-Amiery⁴, Noor Malik Saadoon⁵, Muhammad Faheem Akhtar⁶, Majid S. Jabir^{7*}, Alaa Bassuny Ismael⁸, Ayman A. Swelum^{9*}

1. Faculty of Science and Technology (FST) UKM Universiti/Bangi, Malaysia & College of Medical Engineering, University of Technology- Iraq; P140685@siswa.ukm.edu.my ; Ahmed.j.jasim@uotechnology.edu.iq (A.J..J)
2. Department of Chemical Sciences, Faculty of Sciences and Technology, Universiti Kebangsaan Malaysia, UKM, Bangi,43600, Selangor, Malaysia rahimi@ukm.edu.my (M.R.)
3. UKM — Photonic Technology Research Group, Department of Electrical, Electronic and Systems Engineering, Faculty of Engineering and Built Environment, Universiti Kebangsaan Malaysia, UKM Bangi 43600, Malaysia; dra@ukm.edu.my .
4. Al-Ayen Iraqi University, Dhi Qar, Iraq), dr.ahmed1975@alayen.edu.iq (A.A.A)
5. Center of Nano Technology and Advanced Materials, University of Technology- Baghdad, Iraq; Mae.visit.04@uotechnology.edu.iq
6. Liaocheng Research Institute of Donkey High-Efficiency Breeding and Ecological Feeding, Liaocheng University, Liaocheng 252059, China: faheem@lcu.edu.cn
7. College of Applied Sciences, University of Technology- Baghdad, Iraq; 100131@uotechnology.edu.iq (M.S.J)
8. Department of Clinical Laboratory Sciences, College of Applied Medical Sciences, Taif University, P.O. Box 11099, Taif 21944, Saudi Arabia. Email: alismael@tu.edu.sa
9. Department of Animal Production, College of Food and Agriculture Sciences, King Saud University, Riyadh 11451, Saudi Arabia; aswelum@ksu.edu.sa

Corresponding authors: 100131@uotechnology.edu.iq,
aswelum@ksu.edu.sa

Abstract

Comparing chemically produced zinc oxide nanoparticles (CSZnO-NPs) with green synthesized zinc oxide nanoparticles (ZnO-NPs) made using based red yeast rice (RRY) extract as a reducing and stabilising agent, this study looked at the anticancer potential of Zinc oxide NPs against liver cancer cell line. Zinc acetate dihydrate and sodium hydroxide were utilised as precursors in the chemical synthesis process. The ZnO-NPs that were biosynthesised had flower shapes and an average particle size of 22.1 ± 4.3 nm, as determined by FESEM. In contrast, the CSZnO-NPs had bigger, more irregular structures with a mean size of 37.6 ± 5.1 nm. A spectroscopic analysis of UV-VIS nanoparticles (300-800 nm) revealed unique absorption peaks, while XRD confirmed their crystal structures. Hep-G2 liver cancer cells were used to assess anticancer activity. The cytotoxicity of the green ZnO nanoflowers was much greater than that of the CSZnO-NPs, with an IC₅₀ value of 17.35 µg/mL instead of 22.68 µg/mL. In addition, molecular docking

showed that stable complexes (binding energy: -7.18 kcal/mol; K_i : 5.43 μM) were generated by hydrogen bonding with LYS248, HIS179, PRO249, and LEO180 (bond distances: 2.3-3.3 Å) when ZnO nanoflowers were conjugated with the 3HB5 ligand. These results indicate that ZnO-NPs mediated by red yeast rice offer a more environmentally friendly and long-term viable option for treating liver cancer than traditional chemical production methods. Moreover, they show a quantitatively superior anticancer impact.

Keywords: Zinc oxide Nano flowers; Red yeast rice; anticancer; Hep-G2; Apoptosis; In silico study

1. Introduction

A major cause of cancer-related death worldwide is hepatocellular carcinoma (HCC), the most common form of primary liver cancer. The disease has few treatment options and high recurrence rates; more effective and safer therapeutic strategies must be devised. There are several treatment options for hepatocellular carcinoma, but these options are limited and have a high relapse rate. More effective and safer treatment strategies are needed [1]. Unlike traditional treatments such as surgery, chemotherapy, and radiotherapy, nanotechnology-based interventions are less toxic, do not exhibit drug resistance, and offer a better prognosis. Due to their biocompatibility, specific cytotoxicity, and ability to induce apoptosis via oxidative stress, zinc oxide nanoparticles (ZnO-NPs) have recently garnered significant attention. Several studies have shown that ZnO-NPs possess unique anticancer properties that are superior to other metallic nanoparticles, such as silver and gold, and are also less toxic. Furthermore, the type of synthesis and manufacturing process significantly influences the physical, chemical, and biological properties of zinc oxide nanoparticles (ZnO-NPs). Green synthesis using natural plant extracts offers significant advantages, being environmentally friendly, cost-effective, and biocompatible compared to conventional chemical synthesis methods [2-4]. The combination of enhanced anticancer activity and a sustainable and scalable manufacturing method may make biosynthesized ZnO-NPs a viable therapeutic option for hepatocellular carcinoma, given their synthesis from natural and organic materials.

Zinc nanoparticles are known as a unique materials that have many important applications, especially in medicine [5]. These NPs could

be produced using different techniques and can have quite a variety of shapes, leaves, triangles, rods, spheres, and even 3D flowers [6]. Zinc nanoparticles play key roles in many medical applications, such as drug delivery, dental and cancer treatment, wound healing, and antimicrobial effects [7]. The focus is on the preparation of zinc nanoparticles from red yeast rice (Nanoflowers), a chemical innovation. Understanding the 3D structures of these nanoparticles is important when considering their potential applications in diagnostics [8]. Qualitative evaluation of zinc nanoparticles synthesized from red yeast rice is performed through conventional characterization methods such as UV-Visible spectroscopy (FEG-SEM) and FTIR, and is complemented by XRD analysis. Evaluation of newly synthesized naturally occurring zero-valent zinc nanoparticles compared with conventional zinc nanoparticles demonstrates differences in antioxidant properties, as well as differences in antibacterial and anticancer activity against both Gram-positive and Gram-negative bacteria. However, there are several methods that can be used to evaluate the efficacy of zinc nanoparticles for clinical uses [9].

The size, shape, surface area, crystallinity, and bandgap of nanoparticles significantly impact their optical, biological, catalytic, and surface properties, as demonstrated in recent research. Nanoparticles that are green-synthesised have been documented in many sources, including cow urine, *Rauvolfia tetraphylla* leaves, chamomile extract, spider cobweb, and flowers [10-14]. The results of these studies demonstrate that the antibacterial, photocatalytic, and luminescent properties are significantly influenced by the structural and physicochemical characteristics of the materials. The shown significance of nanoparticle characterisation in biological and medicinal applications, therefore, reinforces the relevance of the current work.

Zinc nanoparticles produced from red yeast rice have potential for medical applications and advancements due to their unique features and potential applications. It is recommended that future research investigate whether zinc nanoparticles obtained from red yeast rice are effective in various clinical settings. Zinc nanoparticles play a crucial role in medical applications, primarily due to their multiple uses and distinct physical and chemical properties. This ability to generate these nanoparticles has drawn attention to their medical utility in the fields of blood, rice, yeast, and other related fields. Zinc nanoparticles have unique properties in drug delivery, and in dentistry as materials for treating dental pulp, cancer

treatment, wound healing, and antibacterial properties [15]. Zinc nanoparticles prepared from red yeast rice (Nanoflowers) have demonstrated their ability to combat multidrug resistance of pathogenic bacteria, as well as exhibit anticancer and antioxidant activity. Furthermore, the potential therapeutic properties of zinc nanoparticles against cancer open up new avenues for further research into cancer treatments [16]. Furthermore, Diagnostic methods include ultraviolet (UV) spectroscopy, field-emission scanning electron microscopy (FESEM), Fourier-transform infrared spectroscopy (FTIR), and X-ray diffraction. can be used to synthesize zinc nanoparticles from red yeast rice. These methods, which utilize the three-dimensional structure of zinc nanoparticles, are extremely useful and improve knowledge of their properties in medical applications [17]. Therefore, zinc nanoparticles are of great interest in the medical sector. Its integration into mainstream healthcare undoubtedly offers countless benefits, given its flexibility, acceptable tolerance to many types of infections, anticipated anti-cancer potential, and excellent biochemical properties. Zinc nanoparticles isolated from rice were prepared and subsequently processed using a red yeast assay. *Monascus purpureus*, commonly known as red yeast rice, was identified as possessing unique physiological properties, which led to this investigation on the manufacture of zinc nanoparticles [18]. The phenolic flavonoids in red yeast rice are among the important bio-reductants in stabilizing the ions of some chemicals in aquatic environments. The use of zinc nanoparticles as a protective layer can increase the synthesis and stability of the material [19]. Studies show that red yeast rice extracts provide sufficient total amount of flavonoid (TFC) and the total amount of phenolic content (TPC), which is key for the environmentally sustainable synthesis of zinc nanoparticles [20,21]. Zinc acetate salts promote the continuous transformation into nanoparticles. Understanding the zonal structure of zinc nanoparticles obtained from red yeast rice facilitates the application of their properties and advantages in therapeutic contexts [22,23]. Consequently, several strategies have been used to regulate the dimensions and configurations of these nanoparticles, resulting in distinct morphologies [24]. The sol-gel synthesis using distinct solvents produced hexagonal rods, spherical particles, and thin sheets, respectively. Microemulsion synthesis produced rectangular structures, rods or wires, and spherical nanoparticles by treating with sodium hydroxide and zinc [25].

The interactions between the macromolecules and polyethylene glycol during the synthesis process affected the structural properties of zinc oxide nanoparticles, resulting in the emergence of new rod-shaped crystals, sheet-like shapes, nanowires, and nanorods at different stages. The morphological differences are crucial for determining the differentiation of zinc nanoparticles produced from purple yeast rice [26]. Furthermore, studies have revealed that the synthesized zinc oxide nanostructures exhibit distinct physicochemical properties suitable for biological applications [27]. The nanoparticle synthesis approach can produce nanoparticles with targeted, specific shapes that induce apoptosis, generate reactive oxygen species, and inhibit the growth of microorganisms and cancer cells. These observations demonstrate the effectiveness of the synthesized zinc nanoparticles as an effective resource for antibacterial and anticancer inhibitory reagents. Therefore, determining the three-dimensional structure of zinc nanoparticles produced from purple yeast rice enhances their potential application for medical purposes [28, 29].

Recent advances in nanomedicine are of significant importance for the environmentally friendly synthesis of metal oxide nanoparticles, particularly zinc oxide, due to their biocompatibility and wide-ranging biomedical applications, which have been extensively researched. This has led to increased research into green synthesis methods using plant extracts, fungi, and microbes as sustainable and alternative approaches to chemical methods, offering advantages such as reduced toxicity, lower cost, and enhanced biological activity. However, despite numerous reports and studies on plant-mediated synthesis and their extracts, little attention has been paid to fermented substrates such as red yeast rice (*Monascus purpureus*), which is rich in phenols, flavonoids, and monakulins, and possesses strong reducing and inhibiting potential. Previous studies have shown that these bioactive compounds enhance the morphology and activity of nanoparticles, especially in therapeutic contexts [30-32]. Therefore, combining the unique biochemical properties of red yeast rice with nanotechnology opens new avenues for producing zinc oxide nanoparticles that combine environmentally friendly synthesis with potential anticancer applications. By linking green synthesis with biomedical significance, this study provides a rationale and evidence-based justification for selecting red yeast rice as a biological model for developing zinc oxide nanoparticles.

Red yeast rice (RYR) was chosen in this study due to its medicinal and biochemical potential and its rich phytochemical composition. Like other plant extracts used in nanoparticle synthesis, RYR contains a wide range of compounds that play a significant role in bioactivity, including flavonoids, alkaloids, terpenoids, phenols, saponins, and cardiac glycosides. These compounds serve multiple purposes, including reducing and stabilizing nanoparticle formation and imparting antioxidant and antimicrobial properties. Previous studies has shown that thorough phytochemical screening is necessary for two reasons: first, to verify the existence of these chemicals; and second, to determine how the biological activities of the synthesized nanoparticles relate to the quantitative and qualitative features of these compounds. Hence, RYR is a valid choice because it aligns with the growing body of research indicating that plant extracts rich in secondary metabolites can be utilised to synthesise eco-friendly nanoparticles. These nanoparticles can enhance antimicrobial and therapeutic outcomes, but only after a thorough phytochemical analysis is conducted, which includes both quantitative estimation and qualitative presence testing.

2. Method and Materials

2.1 Zinc Nanoparticle Synthesis Using Red Rice Yeast

Red rice yeast was agitated at 4,000 rpm and heated to 80 °C in 50 ml of distilled water for 45 minutes; the extract had a pH of 7.3. The extract was separated from the combination of supernatant using Whatman filter paper. Subsequently, 2 ml of the plant extract was combined with 2 ml of 0.5 M zinc acetate, (Sigma-Aldrich, Cat. No. 96459). for a duration of 45 minutes. The mixture has been centrifuged at 5000 rpm for 30 minutes at 4 °C. During the agitation of the solution, 2 M NaOH (Merck, Cat. No. 106498) was incrementally introduced, leading to the appearance of a white precipitate,[21] This reaction was followed by additional stirring for the remaining 2 hours. The mixture was centrifuged for 10 minutes at 4000 rpm and a precipitate formed which needs to be washed with distilled water until the pH level got to 7.2. The collected precipitate was subsequently dried for 2 hours at 80 °C to obtain highly pure ZnO nanoparticles. Particle characterization was done using the following techniques.

2.2 Chemically synthesized ZnO nanoparticles (CSZno-NPs)

2.2 g of NaOH is first dissolved in a beaker of 100 ml of distilled water (~0.55 M), stirred well to dissolve completely. The solution for the zinc precursor (0.27 M) is obtained by adding 5.95g Zinc acetate ($\text{Zn}(\text{CH}_3\text{COO})_2 \cdot 2\text{H}_2\text{O}$) in 100 mL of filtered water. Amount of 0.5-1 g of PVP is also added for stabilization and heated to 60-80°C while being stirred. The alkaline solution (NaOH) is slowly (1-2 ml/min) poured into the hot zinc solution under vigorous stirring. You will immediately see a milky white precipitate when you add (that's $\text{Zn}(\text{OH})_2$ changing to ZnO). Keep hot and stirring until the reaction is over, that is, 1-2 hours. Cool the blend to room temperature without any forced cooling (or maintain at 60°C for 2-4 hours for better crystallization). The precipitate is centrifuged (3000-5000 rpm, 10 min). The resultant precipitate has been centrifuged and rinsed three or four times with distilled water/ethanol to get rid of excess ions and impurities. The precipitate is toasted in a hot oven for 6-12 h at 60-80°C. This leads to the growth of ZnO nanoparticles.

2.3. Characterization of ZnO nanoparticles

Using a Shimadzu UV-1700 spectrometer, which measures absorbance over a wavelength range of 200-800nm, the UV and visible absorbances of the nanoparticles were determined. The anatomical properties of the zinc oxide Nanoparticles have been analyzed utilizing a field scanning electron microscope (FESEM). Zeta potential and FTIR techniques were used for characterization. Finally, the resulting Zinc oxide nanoparticles have been explored by the technique of X-ray diffraction (XRD). The above-mentioned investigations were performed for zinc particles synthesized from red yeast rice and chemically synthesized zinc particle(CSZnO-NPs) .

2.4. Anticancer activity of ZnO nanoparticles (MTT assay)

The ZnO nanoparticle toxicity assay was investigated against Hep-G2 cells purchased from (Sigma). The complete tissue culture medium RPMI-1640 was used to seed cells at a density of 1×10^4 cells per well. Those cells were as follows subjected to varying doses of zinc oxide nanoparticles for 72 hours following the

24-hour period. The cells were exposed to 2 mg/ml of (MTT) solution for three hours. Next, 100 microliters of dimethyl sulfoxide were added. A microplate reader was used to measure each sample's absorbance at a wavelength of 492 nm. For all cytotoxicity experiments, Hep-G2 cells were seeded at a density of 1×10^4 cells per well in 96-well plates, with each experimental condition performed in triplicate. Untreated cells served as the negative control, while cells exposed to known anticancer agents were used as the positive control. These control groups provided baseline comparisons to assess the relative anticancer efficacy of the ZnO nanoparticles.

2.5. Acridine orange/ethidium bromide (AO/EtBr) staining.

Hep-G2 cells were seeded on 12-well plates at a density of 1×10^6 cells/well. After 24 h, zinc oxide nanoparticles were added at IC50. Then, the cells were stained for 2 min with 10 $\mu\text{g/mL}$ of Acridine Orange/Ethidium Bromide. Fluorescence microscopy was used to examine the cells.

2.6. Edu proliferation assay.

In a 96-well plate, Hep-G2 cells were exposed to zinc oxide nano flowers and commercial zinc nanoparticles at different concentrations, respectively, for 24 h. Edu proliferation assay kit was used to examine the cell proliferation. Fluorescence microscopy was used to examine the stained cells (Olympus IX51, Olympus Corporation, Tokyo, Japan).

2.7. Mito tracker staining

The Mito Tracker device was used to label Hep-G2 cells at a final dose of 25 nmol for 60 min to examine mitochondrial release induced by red yeast rice zinc oxide nanoparticles and chemically synthesized zinc nanoparticles. The cells were then exposed to red yeast rice zinc oxide nanoparticles (Nanoflowers) at IC50 and chemically synthesized zinc nanoparticles (CSZno-NPs) at IC50 for 4 h, respectively.

2.8. Cathepsin B staining

Anti-cathepsin B antibodies (Abcam, 1:500) were incubated with Hep-G2 cells after they were treated with zinc oxide nanoflowers and chemically synthesized zinc nanoparticles (CSZno-NPs) at IC₅₀ for 12 h. Then, goat and mouse FITC secondary antibodies were used to stain Hep-G2 cells for fluorescence immunostaining.

2.9. Glutathione (GSH) levels inside cells are analyzed.

The total number of available thiols in liver cancer cells treated with single-walled carbon nanotubes, pink red yeast rice nanoflowers /zinc oxide single-walled carbon nanotubes, and chemically synthesized zinc nanoparticles (CSZno-NPs) was determined by staining the cells. VitaBrite-48™ (VB -- 48™). The experiment was performed in accordance with the manufacturer's guidelines.

2.10. ZnO NPs inhibit Liver Cancer Spheroids

A three-dimensional sphere was created to contrast the consequences of untreated control Hep-G2 cells and liver cancer cells treated via ZnO nanoparticles (zinc oxide nanoparticles) in a 3D cell model. Briefly, two solutions of polyethylene glycol (PEG),(PEG, 35,000 D) And 12.8% dextrin (500,000 D) at a concentration of 5% (w/w) They were generated using the culture media. Into a 6-well plate, one milliliter of 2% (w/v) agarose solution. During refrigeration of the agarose solution, each well was cleaned using sodium phosphate buffer (PBS), after which each well received 1 mL of 5% (w/w) PEG solution. 1×10^6 Hep-G2 Thirty microliters of 12.8% (w/w) aqueous dextrin were used to suspend the cells. ZnO nanoparticles were added to the cells. Fluorescence microscope images were taken to determine the green fluorescence intensity of viable spheres.

2.11. Molecular docking study

Molecular docking is a computational approach that offers valuable insights into the binding interactions between synthesized molecules and the active site of target enzymes. This technique plays a crucial role in evaluating the biological activity of chemical compounds under study, providing a basis for potential structural modifications. In this study, a blind molecular docking was performed on zinc nanoparticles (ZnO NPs) against a selected receptor: 17β-HSD type 1 (Protein

Database ID: 3HB5). The receptor was prepared by removing all associated bonds and solvent molecules. Swiss-PdbViewer (version 4.1.0) (SPDBV) managed the process, which verifies missing protein body fragments and reduces the total energy. The protein database profile of the ZnO NPs was designed using Materials Studio software. This simulation simulated the docking process, and the pairwise interaction energies between the bonds and proteins were calculated using AutoDock 4.2. Nonpolar hydrogen atoms were added to the target proteins, and the spin-orbit bonds of the bonds were determined. Affinity maps (grids) were generated using a $126 \times 126 \times 126$ angstrom grid with a spacing of 1000 angstroms using Autogrid, and docking parameters were adjusted according to the described genetic algorithms. PyMol 3.0 was used to visualize the optimal configurations of silver nanoparticles interacting with the proteins selected in this study.

2.12. Statistical Analysis

GraphPad Prism was used to statistically analyze the data. For statistical analysis, an independent-samples t-test or a one-way analysis of variance (ANOVA) was appropriately applied, followed by post-hoc comparisons between groups using Tukey's test. All experiments were conducted in triplicate, and results were expressed as mean \pm standard deviation (SD). Statistical significance was evaluated using one-way analysis of variance (ANOVA), followed by Tukey's post-hoc test for multiple comparisons. For pairwise comparisons, an independent-samples t-test was applied. A p-value < 0.05 was considered statistically significant. These statistical approaches ensured the reproducibility and reliability of the reported findings.

3. Results

3.1. Zinc NPs characteristics

Optimized chemical processes are applied to prepare zinc nanoparticles from red yeast rice (RYR) for these novel nanostructures. To ensure the highest quality for therapeutic applications, this technique precisely constructs the three-dimensional arrangement of zinc nanoparticles [33]. The quality and properties of the zinc nanoparticles are analyzed using field-efficient scanning electron microscopy (FESCM), X-ray diffraction (XRD), and UV-Vis spectroscopy. The optical properties, i.e., the ability of zinc nanoparticles to absorb and reflect ultraviolet light, are characterized using UV-Vis spectroscopy. As will be demonstrated,

FESCM/XRD can effectively image the surface morphology/structure of the nanoparticles, helping researchers determine the physical properties of the nanoparticles. The structural investigation confirms that the zinc nanoparticles synthesized from red yeast rice (Nanoflowers) possess a well-defined crystalline nature and phase purity as measured by XRD pattern. Comparison of the exostructure properties of chemically synthesized zinc nanoparticles (CSZno-NPs) with red yeast rice nanoflowers (Nanoflowers) revealed significant differences in shape, size, and appearance through XRD, FESEM, and UV-VIS characterizations [34]. These morphologically controlled shapes are demonstrated by current chemical processes, including mechanochemical processing, homogeneous precipitation, and hydrothermal treatment. The final shape and length of the ZnO nanoparticles derived from Nanoflowers depend on the conditions and starting materials used in the synthesis process. Because of quantum size effects, the bandgap energy rises as particle size decreases. Therefore, the process of absorption shifts towards lower wavelengths confirm the reduced size of the ZnO nanoparticles, as shown in **Fig 1**.

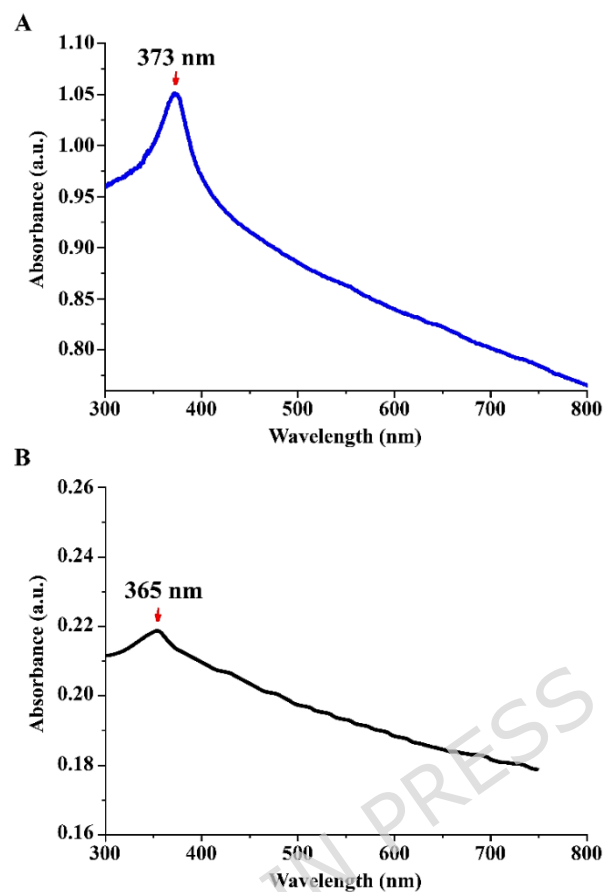


Figure 1: UV-Vis **(A)** ZnO nanoflower; **(B)**. Chemically synthesized zinc nanoparticles (CSZno-NPs)

To further understand the structure and morphology of the synthesised nanoparticles, TEM, and FE-SEM investigations were included. Prior research has highlighted the significance of these methods for confirming particle size, crystallinity, and lattice structures. Spectroscopic and microscopic studies have shown the structural validity of Ag and ZnO nanoparticles synthesised from *Rauvolfia tetraphylla* seed extract, shedding light on their unique shape and biological efficacy [35]. Similarly, TEM analysis revealed that the Ag nanoparticles produced from *Rauvolfia tetraphylla* leaf extract had a spherical shape and an average size of approximately 40 nm. These nanoparticles also exhibit photocatalytic properties and have significant medical applications. [11]. To bolster the current work, such studies should be evaluated, as they demonstrate the significance of high-resolution electron microscopy in nanoparticle characterisation. In addition, the spherical shape and cubic structure of the silver oxide nanoparticles

(Ag₂O NPs) were confirmed by photoluminescence, PXRD, UV-Vis, FTIR, TEM, SEM-EDS, and green synthesis with Cucumis melo seeds. With visible light, the Ag₂O NPs showed potential as photocatalysts for degrading methylene blue, and they were very effective against both Gram-positive and Gram-negative bacteria [36]. FESEM and TEM images showed that these chemically synthesized zinc nanoparticles (CSZnO-NPs) are relatively homogeneous in distribution and have rounded shapes. It is likely that, depending on the starting materials used, standard techniques for making typical zinc oxide nanoparticles can lead to changes in size and shape. For example, zinc nitrate can favor the formation of flower-shaped clusters due to electrostatic attraction, while zinc acetate can create small, bullet-shaped spherical structures that tend to aggregate [37]. Developed zinc oxide nanoparticles (synthesized from red yeast rice) exhibit diverse shapes (nanoflowers), such as nanowires, nanorods, nanotubes, and nanotetragons. Current chemical processes, including mechanochemical treatment, homogeneous precipitation, sol-gel techniques, microemulsion synthesis, and hydrothermal treatment, have demonstrated the ability to control these shapes. [25]. The final shape and length of red yeast-derived zinc nanoparticles depend on the conditions and starting materials used in synthesis [38]. Finally, we can focus on the differences in the external morphology of red yeast-derived zinc nanoparticles, noting that nanoparticles may have a versatile and tunable structure depending on the synthesis process [39,40]. Chemically synthesized zinc nanoparticles (CSZno-NPs) tend to be more spherical as shown in **Fig 2**, while red yeast-derived zinc nanoparticles (nanoflowers) exhibit a wider range of shapes and can be intentionally manufactured for microencapsulation in scientific applications.

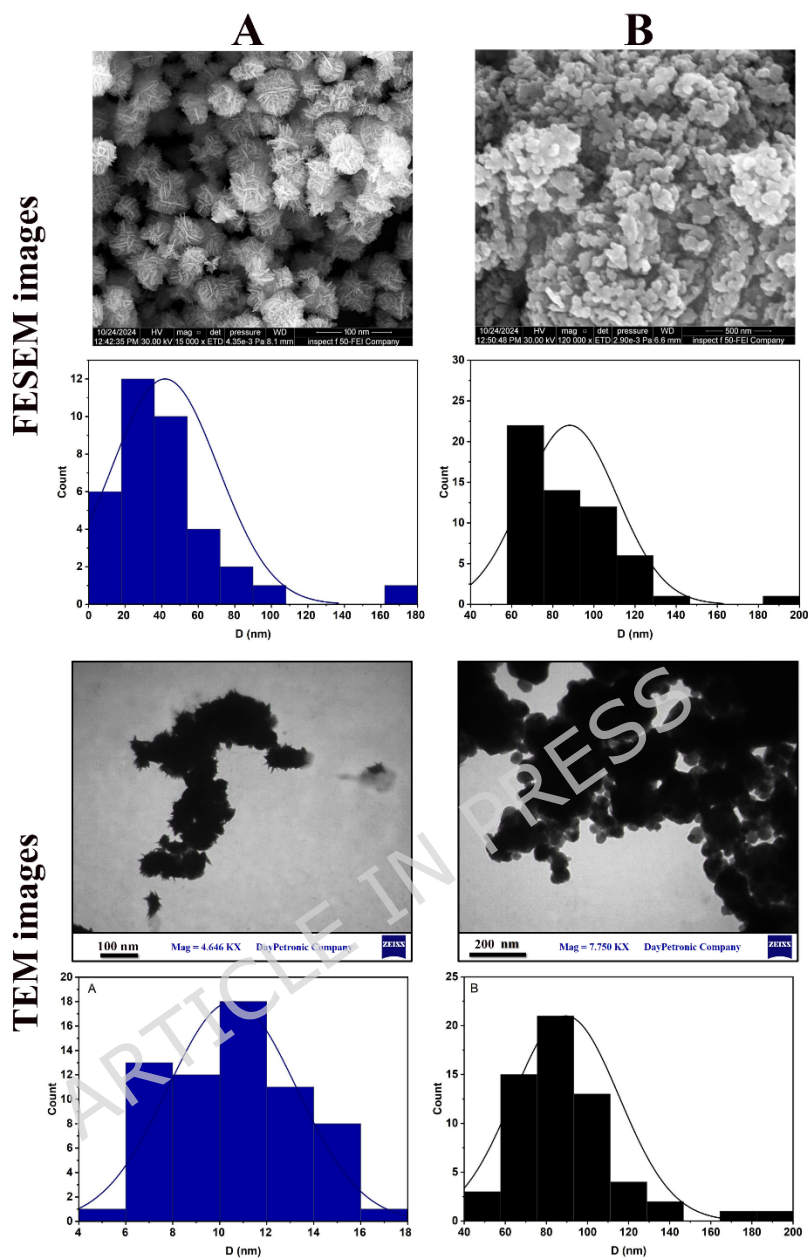


Figure 2: FESEM, and TEM showed Morphology of ZnO Nanoflower (A) and Morphology of chemically synthesized zinc nanoparticles (CSZno-NPs) (B).

Diffraction peaks corresponding to zinc oxide (ZnO) are assigned to the main peaks at angles $2\theta \approx 31.7^\circ$ (100), 34.4° (002), 36.2° (101), 47.5° (102), 56.6° (110), 62.8° (103). Comparison of the exoskeleton properties of chemically synthesized zinc nanoparticles and red yeast rice nanoparticles indicated differences in shape, size, and appearance through XRD characteristics. Slightly wider peaks in **Fig.3 (A)** indicate smaller nanoparticles resulting from biosynthesis from red yeast rice, while narrower peaks in **Fig3 (B)** indicate larger particles or higher crystallinity. Additional peaks appearing at (e.g., at $\approx 27^\circ$ or 38°) in chemically synthesized zinc nanoparticles may indicate impurities such as $\text{Zn}(\text{OH})_2$ or ZnO_3 . The particle shape

is a “nanoflower” structure in **Fig.3 (A)**, where sharper peaks typically appear in the (20) direction due to three-dimensional crystalline aggregation. **Fig.3 (B)**, balanced peaks reflect spherical or irregular shapes. The results suggest that the catalytic and optical efficiency of the smaller particles in Sample A may increase the surface area, enhancing catalytic applications (such as the degradation of pollutants). Biopreparation using red yeast rice **(A)** produces ZnO nanoparticles with smaller sizes, purer crystals, and a distinct structure (nanoflowers) compared to the chemical method **(B)**, potentially giving them advantages in functional applications such as sensors or photocatalysis, as well as in medical applications. (XRD) characteristics, as shown in **Fig 3**. The absence of non-ZnO peaks in the X-ray diffraction (XRD) patterns confirms the crystallinity and purity of the biosynthesized ZnO nanoparticles. No potential impurities, such as zinc hydroxide or zinc carbonate, were observed, indicating the effectiveness of the washing and neutralization steps. The absence of irregular surface deposits in the high-resolution transmission electron microscopy (FESEM) images also supports the effectiveness of our purification protocol.

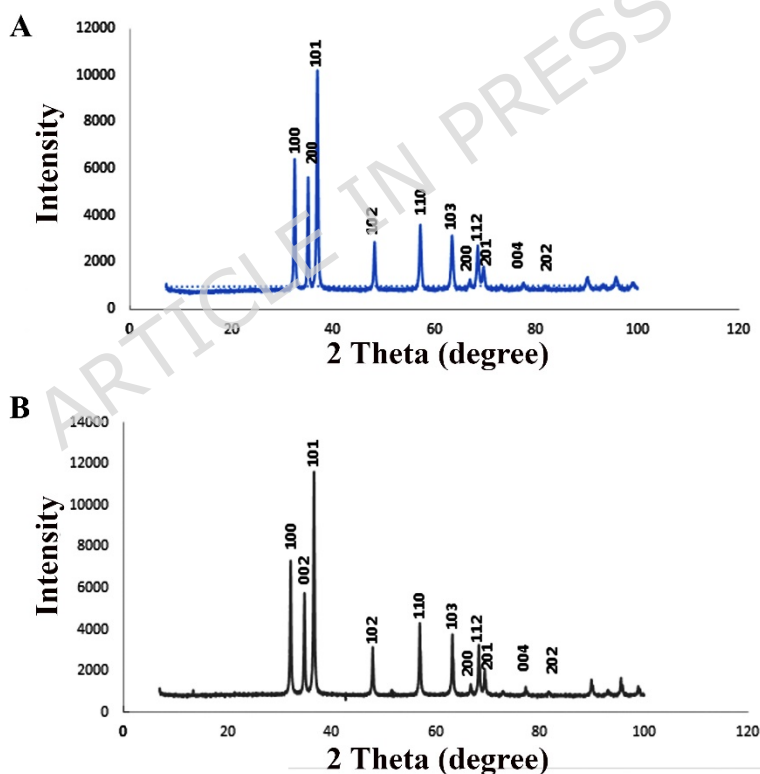


Figure 3: XRD **(A)** ZnO nanoflower; **(B)**. Chemically synthesized zinc nanoparticles (CSZno-NPs)

The crystalline structure of the synthesized ZnO nanoparticles was confirmed via X-ray diffraction (XRD) analysis. The observed diffraction peaks at 2θ values of approximately 31.7° , 34.4° , 36.2° , 47.5° , 56.6° , 62.8° , 66.3° , 67.9° , 69.1° , 72.6° , and

77.0° correspond to the (100), (002), (101), (102), (110), (103), (200), (112), (201), (004), and (202) planes respectively. These peaks match the standard hexagonal wurtzite phase of ZnO, as confirmed by comparison with the Joint Committee on Powder Diffraction Standards (JCPDS) card number 36-1451 [41],[42],[43]. The sharper peaks observed in the green-synthesized ZnO nanoflowers (Figure 3A) suggest higher crystallinity and smaller particle size compared to chemically synthesized ZnO nanoparticles (Figure 3B). The average crystallite size (D) was calculated using the Debye-Scherrer equation:

$$D = \frac{K\lambda}{\beta \cos \theta}$$

where K is the Scherrer constant (0.9), λ is the X-ray wavelength (0.15406 nm), β is the full width at half maximum (FWHM) of the most intense peak in radians, and θ is the Bragg angle. The average crystallite size for the green-synthesized ZnO nanoflowers was estimated to be 19.8 nm, while that of the chemically synthesized ZnO was 28.4 nm. These findings further confirm that green synthesis not only ensures eco-friendliness but also leads to finer nanoparticles with high crystallinity, which are crucial for biomedical activity such as anticancer efficacy [31]. The plane indices have been clearly labeled in the attached XRD plots (Figure 3) as per reviewer's request.

Figure 4 shows the results of the zeta potential tests used to assess the nanoparticles' surface charge and colloidal stability. The zeta potential value of the chemically synthesised ZnO nanoparticles, Figure 4(A), was approximately +5 mV, whereas Figure 4(B) was somewhat higher at around +12 mV, whereas the biosynthesised ZnO nanoflowers. Positive surface charges were observed in both nanoparticle types, which is often beneficial for dispersion stability, as particles repel each other electrostatically. Because phytochemicals from red yeast rice extract serve as capping and stabilising agents, lowering the net surface charge and improving biocompatibility, the green-synthesised ZnO nanoflowers have a substantially lower zeta potential. Water's sharp and narrow distribution peaks indicate colloidal stability, which implies uniform surface charges. The results show that ZnO nanoparticles, whether chemically or biochemically synthesised, are suitable for use in biological applications. However, nanoflowers capped with biomolecules may have an advantage in interacting with cells and exhibiting less aggregation.

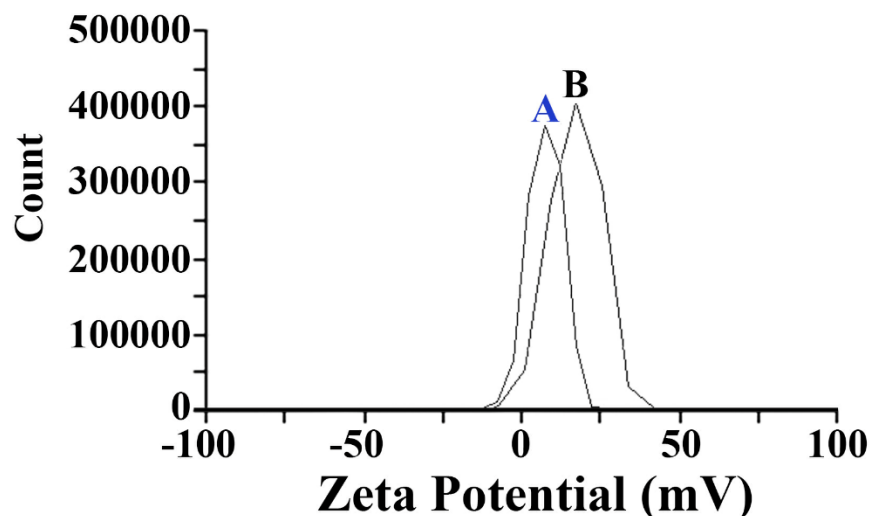


Figure 4: Zeta potential of **(A)** ZnO nanoflower; **(B)**. Chemically synthesized zinc nanoparticles (CSZno-NPs)

Two different methods were used to synthesise ZnO nanoparticles. The absorption peaks at 3678.98 cm^{-1} in ZnO nanoflower are indicative of hydroxyl group O-H stretching vibrations, which may indicate the presence of stabilising substances such as alcohols, phenols, or adsorbed water molecules from plant metabolites. Organic phytochemicals may have C=C or C=N stretching vibrations at 2236.87 cm^{-1} , as shown by the peak at 2869.56 cm^{-1} , which corresponds to C-H stretching vibrations of alkanes. The absorptions support the presence of biomolecules in the stabilisation and capping of nanoparticles at 1789.69 cm^{-1} and 1896.35 cm^{-1} , which may be associated with the C=O stretching vibrations of carbonyl groups found in proteins or flavonoids. The stretching vibrations of C-O are linked to the band at 1113.78 cm^{-1} , whilst the bending of C-H and potential stretching modes are represented by the peaks at 856.64 cm^{-1} and 635.87 cm^{-1} , respectively. The prominent absorption band confirms the effective production of ZnO nanoparticles at 415.08 cm^{-1} , which is attributed to the ZnO stretching vibration. The number of peaks pertaining to organic compounds is lower in CSZnO -NPs showing the chemical synthesis compared to green synthesis (Data not shown).

3.2. Activity of ZnO NPs against cancer

A cytotoxicity test of zinc oxide nanoparticles was performed. Hep-G2 cells were provided by the Iraqi Specialized Laboratory for Medical Genetics and Cancer Research, and were cultured in complete tissue culture medium (RPMI-1640) at a density of 1×10^4 cells per well. Those cells were treated with different doses of (ZnONPs)zinc oxide nanoparticles for 72 hours after a 24-hour break [44]. The cells were exposed to 2 mg/ml of (MTT) solution for three hours. 100 μl of dimethyl sulfoxide was then added. A microplate reader quantified the absorbance of each sample at a wavelength of 492 nm [45]. The EdU test for cellular proliferation included exposing Hep-G2 cells to ZnO nanoparticles for 24 hours at doses IC₅₀ in

a 96-well plate. Cell proliferation was assessed using an EdU proliferation test kit. The stained cells were analysis using a fluorescence microscope. ZnO's cytotoxic nanoparticles on (Hep-G2), cells were evaluated by MTT assay. ZnO nanoparticles exhibited greater effects on Hep-G2 cells than chemically synthesized nanoparticles (CSZno-NPs). ZnO nanoparticles synthesized from red yeast rice (ZnO nanoflowers) considerably reduced the growth of cancer cell lines more than chemically synthesized zinc nanoparticles (CSZno-NPs). The results of the Edu test, as shown in the **figure 5**, confirmed that ZnO nanoparticles synthesized from red yeast rice (ZnO nanoflowers) significantly inhibited the proliferation of Hep-G2 cells more than chemically synthesized zinc nanoparticles (CSZno-NPs). An eco-friendly way to create a variety of metal oxide and metal nanoparticles with regulated size and form is through synthetic processes that use natural plant products and their biocomponents. The results indicated that the ZnO nanoparticles produced from red yeast rice could be used as an effective anticancer therapy for a wide range of malignancies.

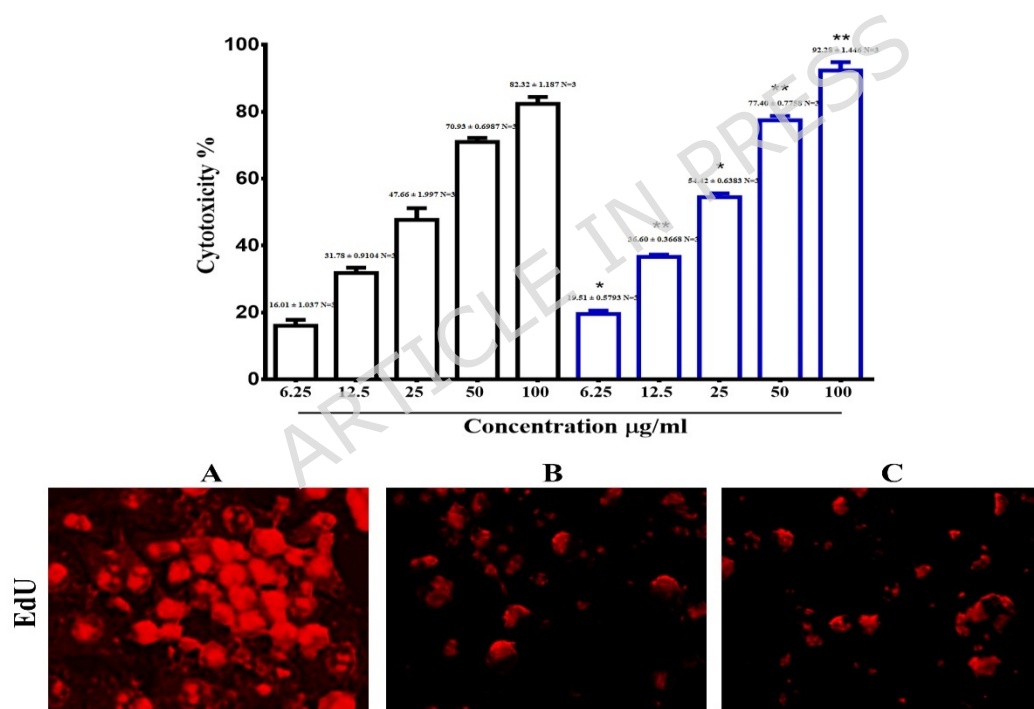


Figure 5: Anticancer efficacy of ZnO nanoparticles against Hep-G2 cells. The upper panel displays the findings of the MTT test, with the black column representing chemically synthesized zinc nanoparticles (CSZno-NPs) and the blue column representing ZnO nanoflowers. (IC₅₀ = 23.98 for µg/ml for (CSZno-NPs) and ZnO 16.44 µg/ml for ZnO nanoflowers). The lower panel displayed the findings of the EdU test. A, Control group of untreated cells. B, Cells were treatment with chemically synthesized zinc nanoparticles (CSZno-NPs). C, Cells were treatment with ZnO nanoflowers. Scale bare 50 µm.

3.2. ZnO NPs stimulate Hep-G2 cells to die through apoptosis.

Twelve-well plates were seeded with Hep-G2 cells (1×10^6 cells/well). ZnO nanoparticles were treated at IC_{50} concentration after 24h. After Following that, the cells were stained for two minutes using $10 \mu\text{g/ml}$ AO/EtBr. The cells were visualized on a fluorescent microscope. The current study demonstrated the dose-dependent cytotoxicity of ZnO nanoparticles in response to the cancerous Hep-G2 cell line, as well as its selectivity for cancer cells. The AO/EtBr staining assays were used to analyze viability of the malignant cell line. For AO/EtBr, ZnO nanoparticles were administered to Hep-G2 cells at an IC_{50} concentration. The untreated control cancer cells had exhibited the AO stain (green) as represented in **Fig. 6(A)**, indicating their viability. **Fig. 6(B)** reflects that CSZno-NPs (chemically synthesized ZnO-NPs, the treated cells (were also stained with yellow-orange, fluorescent dye ethylene bromide (EtBr), and it suggests the dead cells). **Fig. 6(C)** prepared zinc nanoparticles from red yeast rice and found it to be toxic on Hep-G2 cells [46].

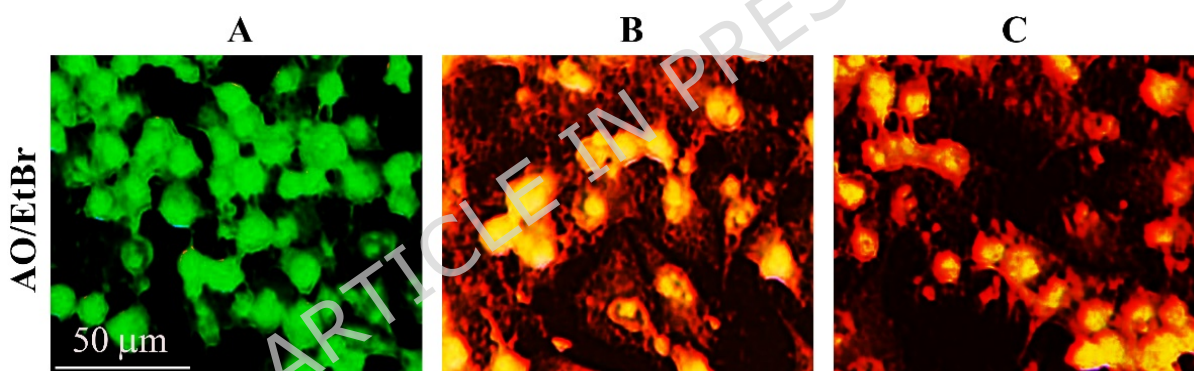


Figure 6: Apoptosis marker in Hep-G2 cells. **(A)**. Control cells that are not treated. **(B)**. chemically synthesized zinc nanoparticles (CSZno-NPs) were applied to the cells. **(C)**, ZnO nanoflowers were applied to the cells. Scale bare $50 \mu\text{m}$.

3.3. Examination of the levels of intracellular glutathione (GSH)

The VitaBright-48TM (VB--48TM) was used to measure the amount of free thiol in Hep-G2 cells [47]. The effect of ZnO NPs with free thiols loadings is presented in **Fig.7**. This experiment was conducted in accordance with manufacturer's instructions. Parameters associated with oxidative stress were monitored to further determine ROS production and redox equilibrium changes induced by the nanoparticles in the treated hepatocellular carcinoma cells. At first, the total free thiol -content was evaluated, with a contribution from

GSH decrease. Since GSH scavenges ROS, it plays a crucial role in maintaining redox homeostasis in cells and is recognized as one of the most important endogenous substances in the defensive system of antioxidants. In reality, the level of its endogenous cellular content is very low resulting with excess oxidative effects on cells which outcome cell death. As seen in **Fig.7**. Hep-G2 cells treated red yeast rice zinc nanoparticles nanoflowers and chemically synthesized zinc nanoparticles (CSZno-NPs led to a critical decrease in GSH, changing cell cytosol from a reducing to an oxidative atmosphere. This was due to alteration in the β -GSH homeostasis. These cell populations of low GSH levels were raised from 25.87% to 62.49% for chemical prepared zinc nanoparticles (CSZno-NPs), and **83.04%** for ZnO nanoflowers as compared to untreated cells.

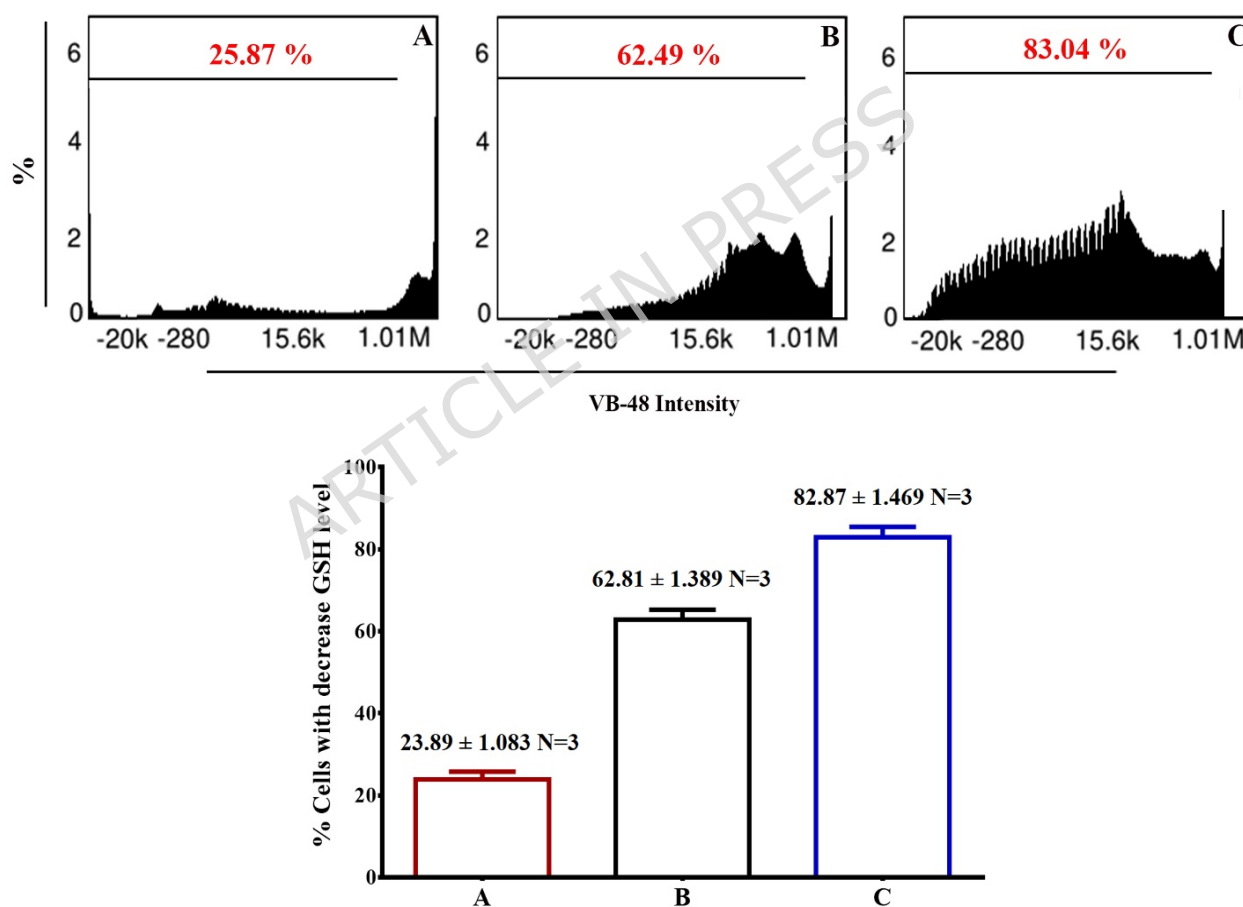


Figure 7: GSH levels in Hep-G2 cells are decreased by Zn O NPs. **(A)**. Manage cells that are not treated. **(B)**. Chemically synthesized zinc nanoparticles (CSZno-NPs), **(C)**. ZnO nanoflowers were applied to the cells.

3.4 Effect of ZnO NPs on Mitochondria

To test mitochondrial release induced by ZnO nanoflower and commercial ZnO nanoparticles The Hep-G2 cells were stained and Mito Tracer at a final concentration of 25 nmol for 60 minutes. Subsequently, cells were subjected to commercial ZnO nanoparticles at IC50 for 4 hours and Nano flower ZnO nanoparticles at IC50 [48]. The results of this test confirmed that the percentage of cancer cells treated increased from 4.06% to 22.65% when using commercial zinc nanoparticles, and in cells treated with zinc oxide nanoparticles manufactured from red rice yeast, from 22.65% to 35.27%. In cancer cells, zinc oxide nanoparticles cause apoptosis in a dose-dependent manner, as seen in **fig. 8**.

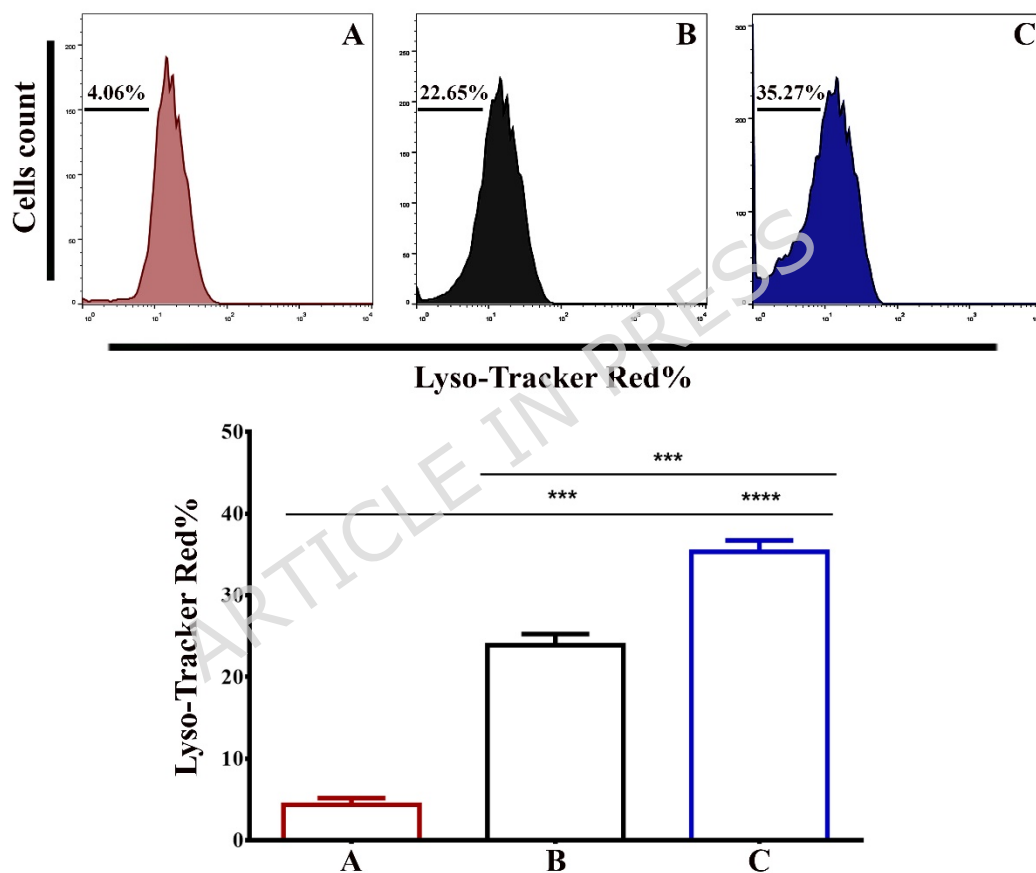


Figure 8: ZnO nanoparticles reduce Lyso-Tracker red in Hep-G2 cells: (A). Control group of untreated cells, (B). Cells were treated with chemically synthesized zinc nanoparticles (CSZno-NPs), and (C). Cells were treatment with ZnO nanoflowers.

3.5 Effect of ZnO NPs in Cathepsin B level

After Zinc oxide nanoparticle therapy (Zno nanoflowers) and chemically synthesized zinc nanoparticles (CSZno-NP s), Hep-G2 cells were treated with anti-cathepsin B antibodies (Abcam, 1:500) for 12 h. Hep-G2 cells were then stained for

immunofluorescence by use of secondary antibodies against goat FITC and mouse FITC [49,50]. To investigate whether lysosomal damage is associated with ZnO nanoparticles causing growth inhibition of Hep-G2 cells, we looked at the lysosomes. Changes of Hep-G2 cells treated with ZnO nanoparticle extract. Our results showed that the lysosomal molecule's intensity of fluorescence was increased after Hep-G2 cells were treated with ZnO nanoparticles of both types, as shown in Fig 9. Hep-G2 cells treated, with ZnO nanoparticles at the IC50 concentration induced lysosomal damage. In biological systems, there are several proteins and enzymes that are crucial in the degradation of lysosomal proteins. One such is cathepsin B, which is discharged into the cell's cytoplasm and causes the integrity of the lysosomal membrane to be compromised in Hep-G2 cells.

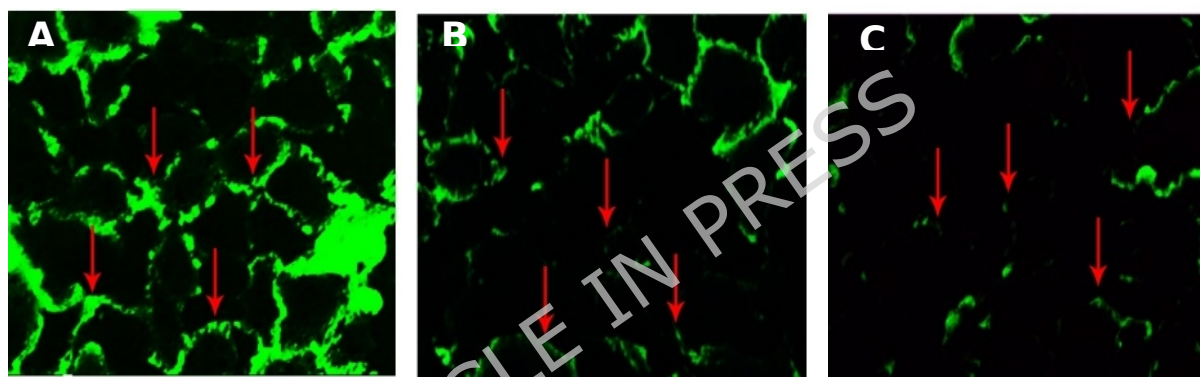


Figure 9: Zn O NPs reduces Cathpsin B in Hep-G2 cells: **A.** Control untreated cells, **B.** Cells were treated chemically synthesized zinc nanoparticles (CSZno-NPs), **C.** Cells were treated with ZnO nanoflowers. Red arrows indicated cathepsin B. Scale bare 50 μm .

3.6 ZnO NPs inhibit Liver Cancer Spheroids

Liver cancer spheroids were inhibited by zinc nanoparticles. To date, Hep-G2 cells in two-dimensional cell cultures have been successfully treated with zinc nanoparticles. However, before analyzing the results of the dual treatment, a more precise knowledge of the tumor environment model is required. Therefore, we tested our proven approach on a three-dimensional tumor cell model. The current study's findings demonstrated that the untreated Hep-G2 cell population contained a very high percentage of viable spheroids. As shown in **Fig.10**, this percentage was significantly lower in the zinc nanoparticle-treated groups. Spheroid aggregation was significantly reduced after zinc nanoparticle treatment. In the three-dimensional cell model, zinc oxide nanoparticles inhibited spheroids in

contrast to the control group, indicating a pertinent therapeutic effect. A greater number of cells were inhibited in the zinc oxide nanoflower treatment compared to the group exposed to chemically synthesized zinc nanoparticles (CSZno-NPs).

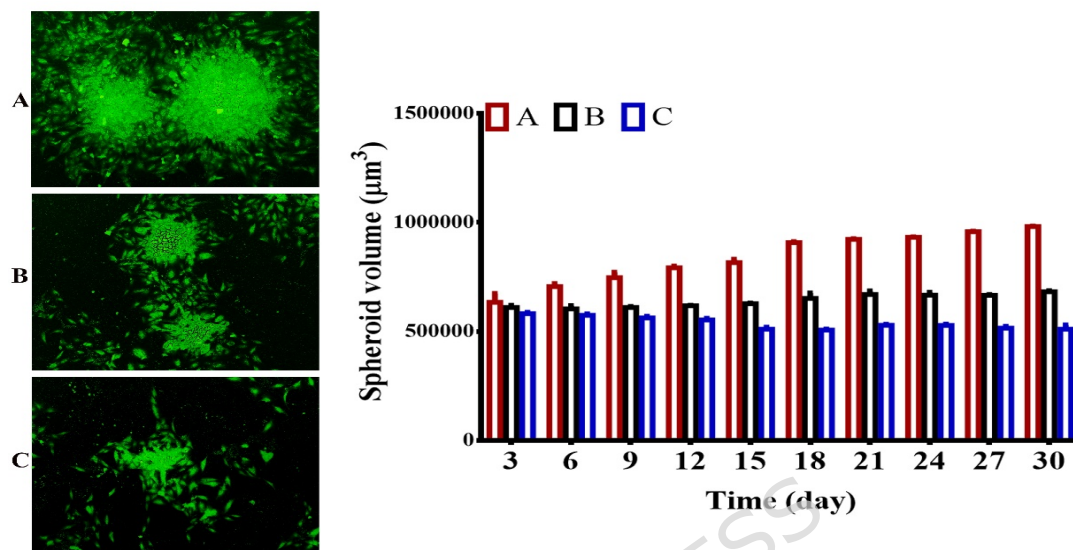


Figure 10: Spheroid value in Hep-G2 cells is decreased by ZnO NPs: **A.** Control untreated, **B.** chemically synthesized zinc nanoparticles (CSZno-NPs). treated cells, **C.** ZnO nanoflowers treated cells.

Although rosette-shaped zinc oxide (ZnO) nanoparticles synthesized utilizing red yeast rice (RYR) showed considerable anticancer activity against Hep-G2 liver cancer cells *in vitro*, there are a number of potential limitations and other explanations to take into account. Leftover bioactive substances from RYR also contribute to the biological activity, rather than only the ZnO nanoparticles, which might explain the reported cytotoxic effects [51]. Cellular absorption and bioactivity may also be affected by variations in physicochemical qualities depending on the production technique [52]. These variables include particle size, surface charge, and aggregation state. The study has some limitations, one of which is that it only used *in vitro* Hep-G2 models, which might not be representative of the complexity *in vivo*. Thorough *in vivo* toxicity evaluations are necessary to establish safety prior to any therapeutic uses, and the processes behind apoptosis induction remain unclear [53]. Finally, it is essential to acknowledge these alternative reasons and limitations, even though preliminary findings on the anticancer potential of ZnO nanoparticles synthesized by RYR were encouraging. Their therapeutic potential and safety can only be fully evaluated through additional *in vivo* research and thorough mechanistic investigations.

3.7. In silico Findings

In this study, molecular docking simulations were employed to evaluate the interaction between zinc oxide nanoparticles (ZnO NPs) and the anticancer receptor (PDB ID: 3HB5) in order to identify the optimal conformations for their interaction, as shown in Figure 11. The results indicate that the free binding energy (ΔG) of zinc oxide nanoparticles interacting with the 3HB5 receptor is -7.18 kcal/mol, demonstrating a strong affinity between the zinc oxide nanoparticles and the cell-derived anticancer receptor. Furthermore, the ΔG values, ranging from -7.06 to -6.10 kcal/mol (as shown in Table 1), suggest that the interaction occurs within a narrow range of binding energies, indicating relatively stable interactions with some variation between different configurations. The inhibition constant (K_i) is another important parameter used to assess the strength of the interaction between zinc oxide nanoparticles and the 3HB5 receptor. The K_i value for the first configuration is 5.43 μmol , indicating a strong inhibitory effect against the receptor. For the other configurations, the K_i increases as the binding energy decreases. For example, the K_i values for the other configurations are 8.22, 13.03, 23.52, and 55.11 μM , indicating weaker inhibition with lower binding energy (as shown in Table 2). Hydrogen-bonding interactions between zinc oxide nanoparticles and the cell receptor were also investigated and identified. This demonstrates that these interactions play a crucial and effective role in binding stability. For example, several hydrogen bonds were observed between the oxygen atom in the bond and the amino groups in the receptor protein, such as LYS248 and HIS179. This type of interaction enhances and contributes to the overall stability of the compound. These interactions suggest the potential for zinc oxide nanoparticles to effectively inhibit receptor activity. Based on molecular docking simulations and detailed free energy analysis of the binding, zinc oxide nanoparticles show promising potential as potent anticancer agents, with the first configuration exhibiting the strongest interaction with the 3HB5 receptor. These findings open up new and broad avenues for exploring zinc oxide nanoparticles as therapeutic agents in cancer treatment and other medical applications.

However, further in vitro and in vivo studies are still needed to confirm their efficacy under current biological conditions.

Table 1: The docking parameters were compared to identify the best conformations of ZnO NPs with the receptor/anticancer (PDB ID: 3HB5).

Parameter	ZnO with 3HB5 \Anticancer
Free energy of binding (Kcal/mol)	-7.18
Range (\pm std dev)	-7.06 to - 6.10
Inhibition constant Ki (μM)	5.43
Ref. RMSD	17.91
Hydrogen bonding and bond lengths	LIG O: LYS248 H, 2.3 A°. LIG O: HIS179 H, 2.3 A°. LIG O: PRO249 H, 2.6, 3.2 A°. LIG O: LEO180 H, 2.3, 2.9, 3.3 A°.

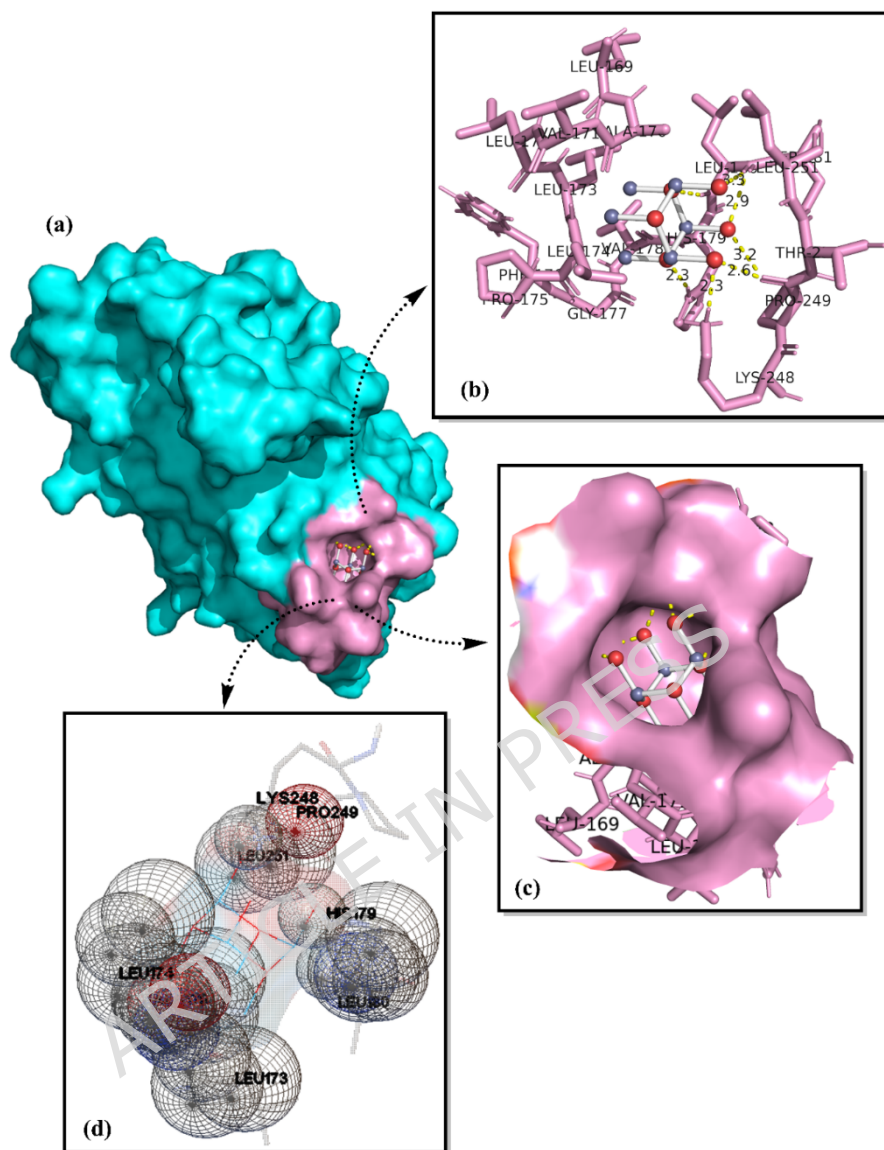


Figure 11: PyMol representations: **(a)** binding pocket of the optimal conformer derived from the docking simulation between ZnO nanoparticles and the 3HB5 receptor. **(B)** Three-dimensional representation of the associated 3HB5 amino acids with the optimal conformer of ZnO nanoparticles. **(C)** Solid surface depiction of the neighboring interacting amino acids with the optimal conformer. **(d)** The protein-ligand complexation is represented using Auto Dock 4.2.

Table 2: Five conformations resulted from the docking simulation reactions between ZnO NPs with the selected receptor\Anticancer (PDB ID: 3HB5)

Conformer's No.	ZnO NPs with 3HB5 receptor\Anticancer	
	Free energy of binding (Kcal/mol)	Inhibition constant Ki
1	-7.18	5.43 uM
2	-6.94	8.22 uM
3	-6.66	13.03 uM
4	-6.31	23.52 uM
5	-5.81	55.11 uM

Zinc oxide (ZnO) is a much sought-after substance with high bioactivity in numerous uses, including as anti-inflammatory, anti-cancer, antioxidant, and antibacterial. Because of their specific capacity to cause cytotoxic effects in cancer cells, Zinc Oxide Nanoparticles (ZnO NPs) show considerable and encouraging potency as an anticancer drug. In cancer cells, ZnO (NPs) induce oxidative stress and the generation of reactive oxygen species (ROS), which may result in cell cycle arrest or death [54]. ZnO NPs' bioactivity against a liver cancer cell line (Hep-G2) cells (PDB: 3HB5) was investigated in this work, following the 1DXO receptor (free energy of binding -6.74 Kcal/mol, inhibition constant Ki 11.48 μ M), 4F20 (free energy of binding -6.31 Kcal/mol, inhibition constant Ki 23.78 μ M), and 1FJ4 (free energy of binding -5.87 Kcal/mol, inhibition constant Ki 49.85 μ M), ZnO NPs demonstrated the best inhibition effect with the 3HB5 receptor (free energy of binding -7.18 Kcal/mol, inhibition constant Ki 5.43 μ M).

4. Discussion

Cancer treatments have historically focused on surgical removal of tumours, chemo, and radiation. Nanotechnology, on the other hand, has introduced novel approaches to enhance the selectivity and effectiveness of cancer treatments. Due to their biocompatibility, specific toxicity towards cancer cells, and ability to trigger apoptosis through multiple pathways, zinc oxide (ZnO) nanoparticles have garnered interest as a potential therapeutic agent for cancer treatment. The vitality of cancer cells can be dramatically affected

by ZnO nanoparticles. Multiple cancer cell lines, including the MCF-7 breast cancer cell line, have been shown to be cytotoxic after exposure to these nanoparticles. Zargarneshad et al. (2022) highlighted the effectiveness of these agents by showing that treatment with 25 µg/mL of ZnO nanoparticles significantly reduced the number of viable MCF-7 cells to less than 10% [55]. Another study further evidences that ZnO nanoparticles preferentially suppress cancer cell development with minimal harm to healthy cells [56]. One of the primary mechanisms by which ZnO nanoparticles induce cancer cell death is through the induction of oxidative stress and the release of reactive oxygen species (ROS). As shown in the MCF-7 breast cancer model [15], (Anjum et al., 2021; Sgn et al., 2023), this mechanism frequently disrupts the mitochondrial membrane potential, which in turn leads to caspase-mediated pathways of cell death [57]. **Table 3** summarized anticancer activity of ZnO NPs which, are prepared in different ways.

Table 3: Anticancer activity of ZnO NPs.

ZnO NP type	Preparation Method	Mechanism	Ref.
ZnO NPs	Zinc acetate+shilajit extract	Nanoparticles of ZnO produce oxidative stress, cellular malfunction, and apoptosis.	[58]
(ZnO-NPs)	Efficient Fabrication of Sol-Gel	(ZnO-NPs) selectively scavenge reactive oxygen species (ROS) to induce apoptosis and inhibit cancer cell growth.	[59]
ZRT- ZnO NPs	ion-carrier (NaOH)	ZRTs induce cancer cell death by producing ROS.	[60]
ZnO NPs	Ultrasound-irradiated Iziphus jujube extract	ROS generation leads to cytotoxicity, apoptosis, and a decrease in cellular defense.	[61]
Rhus coriaria - ZnO NPs	Rhus coriaria synthesizes.	Apoptotic, cell cycle-arresting, and metastasis-inhibiting ZnO NPs.	[62]
Ni/Cu-ZnO NPs	Investigation of Ni/Cu doped ZnO nanoparticles.	The cytotoxic effects of Ni/Cu-ZnO NPs are increased.	[63]

Plant Extract ZnO NPs	Biosynthesis agents from leaves, fruits, seeds, and roots	ZnO NPs' size, shape, and crystallinity enhance therapeutic effects, reduce toxicity.	[64]
Sea lavender ZnO NPs	Synthesis from sea lavender extract.	ROS production leads to cytotoxicity, apoptosis, and a decline in cellular defense.	[65]
ZnO NPs from Thyme Leaves	A green synthesis method utilizing thyme leaves.	Thyme leaf ZnO nanoparticles exhibit dose-dependent cytotoxicity and growth inhibition, with the effect increasing at 450°C.	[66]
ZnO NPs derived from pumpkin seeds	Biotechnological conversion of pumpkin seeds	Extra ROS and oxidative stress cause antiproliferative effects in HCT116 cancer cells	[67]
Bixa Orellana Extract ZnO NPs	Various components of the Bixa Orellana plant	The release of ions affects cell survival. Overcoating decreases cytotoxicity	[68]
CuO - ZnO	Formation of bimetallic nanoparticles	Copper and zinc ions synergistically increase cytotoxicity.	[69]
Nigella sativa-extracted green ZnO NPs	Nigella sativa extract green synthesis. Two-hour 550°C annealing.	Facilitates apoptosis via cellular uptake processes.	[70]
Pure ZnO NP	Bio-assisted synthesis using extracts from <i>E. officinalis</i> and <i>P. granatum</i>	Suppression of cell growth in MCF-7 cells	[71]
ZnO NPs coated with BSA and TEOS were synthesized.	Synthesized and coated ZnO NPs with BSA and TEOS.	These ZnO NPs preferentially kill Caco-2 cells and induce apoptosis. ZnO promoted late apoptosis and G2/M phase arrest, reducing.	[72]
ZnO NP Nanocomposites	Combined with DOX and folic acid	Reduces EAC cell growth and promotes apoptosis	[73]
ZnO NPs	Green synthesis using plants, fungi, and bacteria	ZnO NPs produce ROS, release zinc ions, and induce cancer cell death.	[74]

Clove Bud Extract-ZnO NPs	Syzygium aromaticum (clove) bud extract green synthesis	CBE-ZnO NPs moderately inhibit tongue carcinoma cells (HNO-97). [75]
----------------------------------	---	--

The green synthesis of ZnO nanoflowers using *Monascus purpureus* (Red Yeast Rice) extract offers considerable cost advantages compared to traditional chemical synthesis. The use of natural plant-derived reducing and stabilizing agents eliminates the need for costly surfactants, capping agents (e.g., PVP, CTAB), and hazardous solvents often employed in conventional protocols. For example, the total material cost of the green process, which consists only of distilled water, red yeast rice, and zinc salts, is approximately 30-50% lower than that of chemical synthesis methods, which require additional stabilizers, organic solvents, and more energy-intensive processing. Furthermore, the absence of chemicals and the avoidance of toxic reagents in the green process reduce the need for intensive post-synthesis purification, thus lowering waste management costs and adhering to safety standards. This makes the method not only more environmentally sustainable but also more economically viable for its potential to expand into the production of pharmaceutical, medical, and industrial nanomaterials. The simplicity of the protocol used in the green process also contributes to energy efficiency, as it does not require intense heating or vacuum conditions. These cost advantages, combined with improved biocompatibility, make biosynthesized zinc oxide nanoparticles a promising candidate for resource-efficient biomedical applications.

The principle employed in this study relies on providing strong in vitro and computer simulation evidence of the efficacy of biosynthesized zinc oxide nanoparticles in combating cancer. However, several limitations must be considered. First, the results are limited to Hep-G2 cell culture models, and further in vivo verification using animal models is required to confirm their therapeutic significance and biocompatibility. Second, the phytochemical composition of red yeast rice extracts may vary between batches depending on the culture and processing conditions used, which in turn may affect nanoparticle production and reproducibility. Third, the current work focuses primarily on cancer cell lines, and toxicity testing against normal liver cells and other healthy cells is necessary to establish safety parameters. While the proposed mechanisms for inducing apoptosis and generating reactive oxygen species (ROS) are supported by experimental evidence, alternative explanations, such as indirect metabolic modification by red yeast rice

biomolecules, cannot be ruled out. Addressing these limitations in future studies will enhance the developmental potential of green-synthesized zinc oxide nanoparticles for clinical applications. Assessment of newly synthesized naturally occurring zero-valent zinc nanoparticles compared with conventional zinc nanoparticles proves many differences in their activity like antibacterial, anticancer, and antioxidant properties. Finally, due to their unique properties and potential applications, zinc oxide nanoparticles (ZnO NPs) have garnered significant attention across various sectors. This is achieved by optimizing the physical and biological properties that determine their reactivity and efficacy through various synthesis methods. These articles focused on different forms of zinc oxide nanoparticles, along with their synthesis techniques and associated processes, and focused on the importance of the synthesis process, properties, and biological interactions, including pharmaceutical, and other biological applications [76-81]. Therefore, zinc nanoparticles are excellent in the medical applications. In addition to typical healthcare undoubtedly offers countless benefits, given its flexibility, acceptable tolerance to many types of infections, anticipated anti-cancer potential, anti oxidant, and excellent biochemical properties. In this study, Zinc nanoflowers were prepared using Red yeast rice, and were identified as possessing unique physiological properties and potent anti-cancer activity.

4. Conclusions

In this work, novel rosette-shaped zinc oxide (ZnO) nanoparticles (NPs) prepared using Red yeast rice (RYR) via a green approach were used. The results demonstrated that high efficacy of Zinc oxide nanoparticles against (Hep-G2) liver cancer cells. Interestingly, these nanoparticles showed a remarkable ability to cause apoptosis in liver cancer cells, a key process in cancer therapies. Furthermore, RYR-synthesized ZnO nanoparticles could potentially serve as a novel therapeutic agent for human cancer cells. With an inhibition constant (K_i) of 5.43 μmol and a binding energy of -7.18 kcal/mol, ZnO nanoparticles with the 3HB5 ligand exhibit anticancer potential. At distances between 2.3 and 3.3 Å, critical hydrogen bonds were observed with LYS248, HIS179, PRO249, and LEO180. These interactions suggest that ZnO-3HB5 may be useful in cancer treatment. Overall, the data obtained indicate a higher efficacy for the studied nanoparticles derived from natural sources compared to chemically

synthesized ones, increasing their potential for use in cancer treatment. Finally, future research should investigate the efficacy and mechanisms of action for these nanoparticles in a more precise and diagnostic manner so that they can be used in future medical applications, given that they are derived from natural, non-toxic, and harmless materials. This opens up further prospects for their uses, as well as their suitability for practical applications.

Acknowledgement: The authors appreciate to the University of Technology-Iraq for their support. The authors extend their appreciation to the Ongoing Research Funding Program (ORF-2025-971), King Saud University, Riyadh, Saudi Arabia, for funding this research. Also, the authors extend their appreciation to the fundamental Research Grant Scheme (FRGS), grant number FRGS/1/2024/STG05/UKM/01/2 funded by the Ministry of Higher Education (MOHE), Malaysia Universiti Kebangsaan Malaysia.

Author Contributions: A.J.J., M.S.J., and M.R., Writing Original, Methodology, Investigation, Visualization, Data curation and Formal examination. A.J.J., M.S.J., and M.R.: Main Concept, Data interpretation, and supervision. A.J.J., M.S.J., M.R, B. A. T., A. A. A., N. M. S., M. F. A., A.B.I and A. A. S.: Writing-review and editing. All authors reviewed the manuscript.

Conflicts of Interest: Contributors verify that they have no competing interests.

Data Availability: All data were represented in this article.

References:

1. Chakraborty, E. & Sarkar, D. Emerging Therapies for Hepatocellular Carcinoma (HCC). *Cancers (Basel)*. **14**, 2798 (2022).
2. Khorrami, S., Zarrabi, A., Khaleghi, M., Danaei, M. & Mozafari, M. R. Selective cytotoxicity of green synthesized silver nanoparticles against the MCF-7 tumor cell line and their enhanced antioxidant and antimicrobial properties. *Int. J. Nanomedicine* **13**, 8013-8024 (2018).
3. Khorrami, S., Zarepour, A. & Zarrabi, A. Green synthesis of silver nanoparticles at low temperature in a fast pace with unique DPPH radical scavenging and selective cytotoxicity against MCF-7 and BT-20 tumor cell lines. *Biotechnol. Reports* **24**, e00393 (2019).

4. Khorrami, S. *et al.* An Improved Method for Fabrication of Ag-GO Nanocomposite with Controlled Anti-Cancer and Anti-bacterial Behavior; A Comparative Study. *Sci. Rep.* **9**, 9167 (2019).
5. Carofiglio, M., Barui, S., Cauda, V. & Laurenti, M. Doped zinc oxide nanoparticles: synthesis, characterization and potential use in nanomedicine. *Appl. Sci. (Basel, Switzerland)* **10**, 5194 (2020).
6. Prasad, R. D. *et al.* A review on concept of nanotechnology in veterinary medicine. *ES Food Agrofor.* **4**, 28–60 (2021).
7. Mandal, A. K. *et al.* Current research on zinc oxide nanoparticles: synthesis, characterization, and biomedical applications. *Nanomaterials* **12**, 3066 (2022).
8. Lata, C. *et al.* in *Cereal Dis. nanobiotechnological approaches diagnosis Manag.* 345–370 (Springer, 2022).
9. Jiang, J., Pi, J. & Cai, J. The advancing of zinc oxide nanoparticles for biomedical applications. *Bioinorg. Chem. Appl.* **2018**, 1062562 (2018).
10. Vinay, S. P., Udayabhanu, Nagaraju, G., Chandrappa, C. P. & Chandrasekhar, N. Novel Gomutra (cow urine) mediated synthesis of silver oxide nanoparticles and their enhanced photocatalytic, photoluminescence and antibacterial studies. *J. Sci. Adv. Mater. Devices* **4**, 392–399 (2019).
11. Vinay, S. P., Udayabhanu, Nagarju, G., Chandrappa, C. P. & Chandrasekhar, N. Enhanced photocatalysis, photoluminescence, and anti-bacterial activities of nanosize Ag: green synthesized via Rauvolfia tetraphylla (devil pepper). *SN Appl. Sci.* **1**, 477 (2019).
12. Vinay, S. P., Alharthi, F. A., Udayabhanu, Alsahme, A. & Nagaraju, G. Hydrothermal synthesis of Ag/rGO@CTFE nanocomposite as a promising photocatalyst for degradation action. *J. Mol. Struct.* **1228**, 129722 (2021).
13. Vinay, S. P., Udayabhanu, Nagaraju, G., Chandrappa, C. P. & Chandrasekhar, N. Hydrothermal synthesis of gold nanoparticles using spider cobweb as novel biomaterial: Application to photocatalytic. *Chem. Phys. Lett.* **748**, 137402 (2020).
14. s p, V., Udayabhanu, U., G, N., Lalithamba, H. S. & N, C. Plant-mediated green synthesis of Ag nanoparticles using Rauvolfia tetraphylla (L) flower extracts: Characterization, biological activities, and screening of the catalytic activity in formylation reaction. *Sci. Iran.* **27**, 3353–3366 (2020).
15. Anjum, S. *et al.* Recent advances in zinc oxide nanoparticles (ZnO NPs) for cancer diagnosis, target drug delivery, and treatment. *Cancers (Basel)*. **13**, 4570 (2021).
16. Ferrag, C. Development of Nanocomposite Gels for Electrochemical Sensors and Energy Applications. at (2023)
17. El-Sayed, E.-S. R., El-Sayyad, G. S., Abdel-Fatah, S. S., El-Batal, A. I. & Boratyński, F. Novel nanoconjugates of metal oxides and natural red pigment

- from the endophyte *Monascus ruber* using solid-state fermentation. *Microb. Cell Fact.* **23**, 259 (2024).
18. Irede, E. L. *et al.* Cutting-edge developments in zinc oxide nanoparticles: synthesis and applications for enhanced antimicrobial and UV protection in healthcare solutions. *RSC Adv.* **14**, 20992–21034 (2024).
 19. Mostafa, H., Airouyuwa, J. O. & Maqsood, S. A novel strategy for producing nano-particles from date seeds and enhancing their phenolic content and antioxidant properties using ultrasound-assisted extraction: A multivariate based optimization study. *Ultrason. Sonochem.* **87**, 106017 (2022).
 20. Khan, I., Saeed, K. & Khan, I. Nanoparticles: Properties, applications and toxicities. *Arab. J. Chem.* **12**, 908–931 (2019).
 21. ADEBARE, J. A. BIOETHANOL PRODUCTION FROM PRETREATED SUGARCANE BAGASSE UNDER OPTIMISED CONDITIONS USING SELECTED FUNGI. at (2021)
 22. Younas, Z. *et al.* Mechanistic approaches to the application of nano-zinc in the poultry and biomedical industries: A comprehensive review of future perspectives and challenges. *Molecules* **28**, 1064 (2023).
 23. Wu, Z., Yang, S. & Wu, W. Shape control of inorganic nanoparticles from solution. *Nanoscale* **8**, 1237–1259 (2016).
 24. Singh, T. A. *et al.* A state of the art review on the synthesis, antibacterial, antioxidant, antidiabetic and tissue regeneration activities of zinc oxide nanoparticles. *Adv. Colloid Interface Sci.* **295**, 102495 (2021).
 25. Mousavi, S. M. *et al.* Shape-controlled synthesis of zinc nanostructures mediating macromolecules for biomedical applications. *Biomater. Res.* **26**, 4 (2022).
 26. Jin, S.-E. & Jin, H.-E. Antimicrobial activity of zinc oxide nano/microparticles and their combinations against pathogenic microorganisms for biomedical applications: From physicochemical characteristics to pharmacological aspects. *nanomaterials* **11**, 263 (2021).
 27. Kadhim, A. A. *et al.* Investigating the effects of biogenic zinc oxide nanoparticles produced using papaver somniferum extract on oxidative stress, cytotoxicity, and the induction of apoptosis in the THP-1 cell line. *Biol. Trace Elem. Res.* **201**, 4697–4709 (2023).
 28. Neamah, S. A., Albukhaty, S., Falih, I. Q., Dewir, Y. H. & Mahood, H. B. Biosynthesis of Zinc Oxide Nanoparticles Using *Capparis spinosa* L. Fruit Extract: Characterization, Biocompatibility, and Antioxidant Activity. *Appl. Sci.* **13**, (2023).
 29. Altammar, K. A. A review on nanoparticles: characteristics, synthesis, applications, and challenges. *Front. Microbiol.* **14**, 1155622 (2023).
 30. Vinay, S. P., Chandrasekhar, N. & Chandrappa, C. P. Eco-friendly approach for the green synthesis of silver nanoparticles using flower extracts of

- Sphagneticola trilobata and study of antibacterial activity. *Int. J. Pharm. Biol. Sci* **7**, 145-152 (2017).
31. Chandrasekhar, N. & Vinay, S. P. Yellow colored blooms of *Argemone mexicana* and *Turnera ulmifolia* mediated synthesis of silver nanoparticles and study of their antibacterial and antioxidant activity. *Appl. Nanosci.* **7**, 851-861 (2017).
 32. Vinay, S. P. & Chandrasekhar, N. Characterization and green synthesis of silver nanoparticles from *Plumeria* leaves extracts: study of their antibacterial activity. *IOSR-JAC* **10**, 57-63 (2017).
 33. Raha, S. & Ahmaruzzaman, M. ZnO nanostructured materials and their potential applications: progress, challenges and perspectives. *Nanoscale Adv.* **4**, 1868-1925 (2022).
 34. Malik, P., Rani, R., Khan, S., Fernandes, D. & Mukherjee, T. K. Green Essence of Plant Resources Capped Zinc Oxide Nanoparticles: Renewable Distinctions, Size-Shape-Modulated Physicochemical Diversity and Emerging Biomedical-Environmental Usefulness. *Part. Part. Syst. Character.* **42**, 2400145 (2025).
 35. Vinay, S. P. & Chandrasekhar, N. Structural and Biological Investigation of Green Synthesized Silver and Zinc Oxide Nanoparticles. *J. Inorg. Organomet. Polym. Mater.* **31**, 552-558 (2021).
 36. Vinay, S. P. *et al.* Facile combustion synthesis of Ag₂O nanoparticles using cantaloupe seeds and their multidisciplinary applications. *Appl. Organomet. Chem.* **34**, e5830 (2020).
 37. Ali, A., Phull, A.-R. & Zia, M. Elemental zinc to zinc nanoparticles: Is ZnO NPs crucial for life? Synthesis, toxicological, and environmental concerns. *Nanotechnol. Rev.* **7**, 413-441 (2018).
 38. Ibrahim, A. B. M. & Mahmoud, G. A. Chemical-vs sonochemical-assisted synthesis of ZnO nanoparticles from a new zinc complex for improvement of carotene biosynthesis from *Rhodotorula toruloides* MH023518. *Appl. Organomet. Chem.* **35**, e6086 (2021).
 39. Harish, V. *et al.* Cutting-edge advances in tailoring size, shape, and functionality of nanoparticles and nanostructures: A review. *J. Taiwan Inst. Chem. Eng.* **149**, 105010 (2023).
 40. Terna, A. D., Elemike, E. E., Mbonu, J. I., Osafile, O. E. & Ezeani, R. O. The future of semiconductors nanoparticles: Synthesis, properties and applications. *Mater. Sci. Eng. B* **272**, 115363 (2021).
 41. Vinay, S. P., Sumedha, H. N., Shashank, M., Nagaraju, G. & Chandrasekhar, N. In-vitro antibacterial, antioxidant and cytotoxic potential of gold nanoparticles synthesized using novel *Elaeocarpus ganitrus* seeds extract. *J. Sci. Adv. Mater. Devices* **6**, 127-133 (2021).
 42. Vinay, S. P., Udayabhanu, Nagaraju, G., Chandrappa, C. P. & Chandrasekhar,

- N. *Rauvolfia tetraphylla* (devil pepper)-mediated green synthesis of Ag nanoparticles: applications to anticancer, antioxidant and antimitotic. *J. Clust. Sci.* **30**, 1545–1564 (2019).
43. Vinay, S. P., Udayabhanu, Nagaraju, G., Chandrappa, C. P. & Chandrasekhar, N. A novel, green, rapid, nonchemical route hydrothermal assisted biosynthesis of Ag nanomaterial by bluishwood berry extract and evaluation of its diverse applications. *Appl. Nanosci.* **10**, 3341–3351 (2020).
 44. Mohammed, T. J. & Al-Shibly, M. K. Therapeutic Effect of Biosynthesis of Selenium Nanoparticles on Enhancing Apoptosis Induction and Cell Lines Arrest in MCF-7 Breast Cancer Cell Lines. *J. Nanostructures* **13**, 796–805 (2023).
 45. Carreno, E. A. *et al.* Considerations and technical pitfalls in the employment of the MTT assay to evaluate photosensitizers for photodynamic therapy. *Appl. Sci.* **11**, 2603 (2021).
 46. Jyothish, B. & Jacob, J. In vitro antiproliferative and G0/G1 cell cycle arrest in human lung carcinoma cells by Ag doped zinc ferrite nanoparticles. *Inorg. Chem. Commun.* **153**, 110869 (2023).
 47. Jabir, M. S. *et al.* Functionalized SWCNTs@ Ag-TiO₂ nanocomposites induce ROS-mediated apoptosis and autophagy in liver cancer cells. *Nanotechnol. Rev.* **12**, 20230127 (2023).
 48. Sasaki, D., Abe, J., Takeda, A., Harashima, H. & Yamada, Y. Transplantation of MITO cells, mitochondria activated cardiac progenitor cells, to the ischemic myocardium of mouse enhances the therapeutic effect. *Sci. Rep.* **12**, 4344 (2022).
 49. Jun, H.-K., Jung, Y.-J., Ji, S., An, S.-J. & Choi, B.-K. Caspase-4 activation by a bacterial surface protein is mediated by cathepsin G in human gingival fibroblasts. *Cell Death Differ.* **25**, 380–391 (2018).
 50. Hu, G. *et al.* Effects of matrine in combination with cisplatin on liver cancer. *Oncol. Lett.* **21**, 66 (2021).
 51. El-Saadony, M. T. *et al.* Green synthesis of zinc oxide nanoparticles: preparation, characterization, and biomedical applications-a review. *Int. J. Nanomedicine* 12889–12937 (2024).
 52. Nandhini, J., Karthikeyan, E. & Rajeshkumar, S. Green synthesis of zinc oxide nanoparticles: eco-friendly advancements for biomedical marvels. *Resour. Chem. Mater.* **3**, 294–316 (2024).
 53. Sanaeimehr, Z., Javadi, I. & Namvar, F. Antiangiogenic and antiapoptotic effects of green-synthesized zinc oxide nanoparticles using *Sargassum muticum* algae extraction. *Cancer Nanotechnol.* **9**, 3 (2018).
 54. Khan, M. J., Ahmad, A., Khan, M. A. & Siddiqui, S. Zinc oxide nanoparticle induces apoptosis in human epidermoid carcinoma cells through reactive oxygen species and DNA degradation. *Biol. Trace Elem. Res.* **199**, 2172–2181

- (2021).
55. Zargarnezhad, M., Mirbahari, S. N. & Ahmadi, R. The Cytotoxic Effects of Zinc Oxide Nanoparticles on SW480 Cell Lines and Measurement of Nitric Oxide in Cell Culture Medium. *Jentashapir J. Cell. Mol. Biol.* **13**, 1-7 (2022).
 56. Ibraheem, S., Kadhim, A. A., Kadhim, K. A., Kadhim, I. A. & Jabir, M. Zinc Oxide Nanoparticles as Diagnostic Tool for Cancer Cells. *Int. J. Biomater.* **2022**, (2022).
 57. Son, N. N., Thanh, V. M. & Huong, N. T. Anticancer Activities of Zinc Oxide Nanoparticles Synthesized Using Guava Leaf extract. *ChemistrySelect* **8**, e202303214 (2023).
 58. Perumal, P. *et al.* Green synthesis of zinc oxide nanoparticles using aqueous extract of shilajit and their anticancer activity against HeLa cells. *Sci. Rep.* **14**, 2204 (2024).
 59. Hadi, A. J. *et al.* Antibacterial and Anticancer Properties of Zinc Oxide Nanoparticles : A Review of Current Advances and Future Directions. **5**, 60-87 (2025).
 60. Aljohar, A. Y. *et al.* Anticancer effect of zinc oxide nanoparticles prepared by varying entry time of ion carriers against A431 skin cancer cells in vitro. *Front. Chem.* **Volume 10**, (2022).
 61. Mousa, A. B., Moawad, R., Abdallah, Y., Abdel-Rasheed, M. & Zaher, A. M. A. Zinc oxide nanoparticles promise anticancer and antibacterial activity in ovarian cancer. *Pharm. Res.* **40**, 2281 (2023).
 62. Mongy, Y. & Shalaby, T. Green synthesis of zinc oxide nanoparticles using Rhus coriaria extract and their anticancer activity against triple-negative breast cancer cells. *Sci. Rep.* **14**, 13470 (2024).
 63. Ayub, H. *et al.* Enhanced anticancer and biological activities of environmentally friendly Ni/Cu-ZnO solid solution nanoparticles. *Heliyon* **10**, (2024).
 64. Al-darwesh, M. Y., Ibrahim, S. S. & Mohammed, M. A. A review on plant extract mediated green synthesis of zinc oxide nanoparticles and their biomedical applications. *Results Chem.* **7**, 101368 (2024).
 65. Naiel, B., Fawzy, M., Halmy, M. W. A. & Mahmoud, A. E. D. Green synthesis of zinc oxide nanoparticles using Sea Lavender (*Limonium pruinosum* L. Chaz.) extract: characterization, evaluation of anti-skin cancer, antimicrobial and antioxidant potentials. *Sci. Rep.* **12**, 20370 (2022).
 66. Karam, S. T. & Abdulrahman, A. F. Green Synthesis and Characterization of ZnO Nanoparticles by Using Thyme Plant Leaf Extract. *Photonics* **2022**, *9*, 594. at (2022)
 67. Kadir, N. H. A. *et al.* Evaluation of the Cytotoxicity, Antioxidant Activity, and Molecular Docking of Biogenic Zinc Oxide Nanoparticles Derived From Pumpkin Seeds. *Microsc. Res. Tech.* **87**, 602-615 (2023).

68. Gharpure, S., Yadwade, R. & Ankamwar, B. Non-Antimicrobial and Non-Anticancer Properties of ZnO Nanoparticles Biosynthesized Using Different Plant Parts of *Bixa Orellana*. *Acs Omega* **7**, 1914-1933 (2022).
69. Sarani, M. *et al.* Biosynthesis of ZnO, Bi₂O₃ and ZnO–Bi₂O₃ Bimetallic Nanoparticles and Their Cytotoxic and Antibacterial Effects. *Chemistryopen* **13**, (2024).
70. Fakhar-e-Alam, M. *et al.* Antitumor activity of zinc oxide nanoparticles fused with green extract of *Nigella sativa*. *J. Saudi Chem. Soc.* **28**, 101814 (2024).
71. Akhtar, M. J., Alhadlaq, H. A., Alshamsan, A., Khan, M. A. M. & Ahamed, M. Aluminum Doping Tunes Band Gap Energy Level as Well as Oxidative Stress-Mediated Cytotoxicity of ZnO Nanoparticles in McF-7 Cells. *Sci. Rep.* **5**, (2015).
72. Ahamed, M., Akhtar, M. J., Khan, M. A. M. & Alhadlaq, H. A. Enhanced Anticancer Performance of Eco-Friendly-Prepared Mo-ZnO/Rgo Nanocomposites: Role of Oxidative Stress and Apoptosis. *Acs Omega* **7**, 7103-7115 (2022).
73. Badawy, M. M. M., Salah, M. & Abdel-Hamid, G. R. Anticancer Approach of Zinc Oxide Nanocomposite Prepared by Gamma Radiation via Induction of Apoptosis and PGC-1 α Pathways in Hepatocellular Carcinoma in Rats. *Appl. Organomet. Chem.* **38**, (2023).
74. Hamrayev, H., Shameli, K. & Korpayev, S. Green Synthesis of Zinc Oxide Nanoparticles and Its Biomedical Applications: A Review. *J. Res. Nanosci. Nanotechnol.* **1**, 62-74 (2021).
75. Hussien, N. A., Khalil, M. A. E. F., Schagerl, M. & Ali, S. S. Green Synthesis of Zinc Oxide Nanoparticles as a Promising Nanomedicine Approach for Anticancer, Antibacterial, and Anti-Inflammatory Therapies. *Int. J. Nanomedicine* 4299-4317 (2025).
76. Evawati, K. & Sutoyo, S. Synthesis and Characterization of ZnO Nanoparticles using the Duwet (*Syzygium cumini*) Leaves Extract as Bioreductor. *J. Pijar Mipa* **20**, 168-172 (2025).
77. Fatoni, A., Afrizal, M. A., Rasyad, A. A. & Hidayat, N. i. ZnO Nanoparticles and Its Interaction With Chitosan : Profile Spectra and Their Activity Against Bacterial. *JKPK (Jurnal Kim. dan Pendidik. Kim.* **6**, 216 (2021).
78. Kumar, R. *et al.* Synthesis and characterization of ZnO Nanoparticles and its application by Sol-Gel Method. 1-9 (2023).
79. Gond, A. K. *et al.* Fabrication and Physiochemical Characterization of Zinc Oxide Nanoparticles via Citric Assisted Auto Combustion Synthesis. *Curr. Nanomater.* **10**, 86-91 (2025).
80. Chandrappa, K. G. & Venkatesha, T. V. Electrochemical synthesis and photocatalytic property of zinc oxide nanoparticles. *Nano-Micro Lett.* **4**, 14-24 (2012).

81. Koli, K., Rohtela, K. & Meena, D. Comparative Study and Analysis of Structural and Optical Properties of Zinc Oxide Nanoparticles using Neem and Mint Extract prepared by Green synthesis method. *IOP Conf. Ser. Mater. Sci. Eng.* **1248**, 012065 (2022).

ARTICLE IN PRESS